Double-directional Superresolution Radio Channel Measurements

Ernst Bonek[1,2], Helmut Hofstetter[2], Christoph F. Mecklenbräuker[2], Martin Steinbauer[1]
[1] *Technische Universität Wien, Gusshausstr. 25-29, A-1040 Vienna, Austria.*
[2] *Forschungszentrum Telekommunikation Wien (ftw.), Donau-City Str. 1, A-1220 Vienna, Austria.*
ernst.bonek@tuwien.ac.at

Abstract

The paper describes measurements of radio propagation at 2 and 5 GHz in urban environments in Vienna, Austria, and Ilmenau, Germany, and in a rural highway environment near Salzburg, Austria, taken with virtual and physical antenna arrays. Multiple antenna elements at both the base and the mobile stations permit, by estimation with superresolution algorithms, evaluation of directions-of-arrival and directions-of-departure.

We aim at a high-precision deterministic full 3-D characterization of the mobile radio channel and succeed in yielding delay, azimuth and elevation of individual multipath components. Comparison with site-maps will allow tracking up to third-order reflections/scattering, thus questioning the applicability of the popular single-bounce models for mobile radio propagation.

We introduce a global measure, the multipath component separation, to describe how well an environment lends itself to smart antenna application.

The channel-state knowledge at the receiver alone, or both at the receiver and the transmitter, bears great impact on the achievable capacity of the current MIMO (multiple-input multiple-output) systems. Our approach to measurement and evaluation forms a solid basis for the calculation of the MIMO capacity in specific environments.

Motivation

We have three motives for carrying out double-directional radio channel measurements: First, a highly precise characterization of the mobile radio channel becomes available when this type of measurements is combined with high-resolution parametric methods. We expect answers to questions like: is reflection, diffraction or scattering the dominant propagation mechanism in urban or office environments? What is more important: over-the-roof or around-the-corner propagation? Comparison with maps will show that up to third-order reflections/scattering can be traced, a result that seriously questions the applicability of the popular single-bounce models in mobile radio propagation. The results will benefit the improvement of ray-tracing algorithms and site-specific network planning.

Second, knowledge of the double-directional radio channel is a prerequisite to exploit the highly current MIMO (multiple-input multiple-output) systems, proposed to enhance the transmission capacity of radio links by orders of magnitude. Whereas a number of interesting theoretical MIMO channel models have been put forward recently, very few measurements accurately describing these channels have been published. In fading channels, the "capacity" itself becomes a random variable (instantaneous capacity). Determining its distribution and related quantities (outage capacity) might require measurements of many realizations in one and the same environment. We would like to characterize the environment by a single measurement run, and independently of the equipment used for the measurement (including the antenna arrays itself).

Third, a more far-reaching goal is site-specific deployment of radio systems, based on an initial double-directional measurement. Just imagine the considerable savings in transmitted power and in system self-interference by transmitting only in the directions where one can be

sure that the signal will be actually received, but will not interfere other mobiles in the cell or system.

Deterministic or stochastic channel models?

Propagation is at the heart of radio communications. It sets the ultimate limits for the transmission speed and throughput of any system built upon radio. Given the obvious attractiveness of mobile radio on one hand, and the complexity of the radio channel on the other, it is clear that good propagation models for electromagnetic waves are needed for both the development and the deployment of the novel MIMO systems envisaged. These systems have multiple antennas at each end of the link, i.e. at the receive and the transmit side. Ideally, independent, orthogonal data transmission channels are set up between the individual antenna elements to maximize transmission capacity.

Stochastic channel models are state of the art for system design and for testing of terminals. Their implementation must be simple and allow fast simulation of systems or part of systems (e.g. receiver algorithms). Whatever environments, situations and fields of application of a system have been included in the mix for the stochastic channel model, the choice of this mix will influence the statistics. Using such a stochastic channel model in system optimisation yields a system that is optimum on average. But in a specific environment, the system will not be optimal, unless it exploits the properties of this very specific environment. We will show that, for MIMO systems, we can supply full knowledge of the main propagation paths determined by the environment.

We do not denounce stochastic channel models in general. Such models have been proposed by e.g. Pajusco [1] for directional channels, Bölcskei et al. [2] and Bach Andersen [3] for MIMO channels. They rely on such concepts as angular spread as seen from the antenna arrays. Scatterers are assumed numerous and randomly distributed. Our deterministic approach to the description of a specific environment, where double-directional channel measurements have been carried out, is only the basis for further stochastic considerations. One note of caution toward supporters of stochastic channel modelling, however, is in place right now: The popular assumption of wide-sense stationary uncorrelated scattering (WSS-US) [4] will fail most probably in directional channel models [5]. The assumption of an infinite number of scatterers is difficult to justify for each delay bin considered [6], but is usually not questioned any further. The situation is aggravated if we switch to directional stochastic channel models: there should be a large number of scatterers in each direction given by a certain value of azimuth and elevation, for each delay bin. This is unrealistic. With increasing angular resolution, the number of scatterers per delay-angle bin will become smaller and smaller, and eventually a single multipath component will remain. Figure 1 illustrates this situation. It shows a modification of the channel model Vehicular A that ITU recommended for IMT 2000 candidate system evaluation [7], where Pajusco extended it to include a spatial component [1].

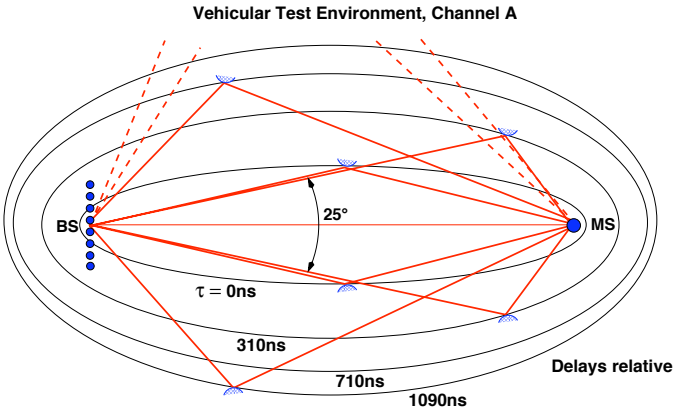

Figure 1: Vehicular A channel model for IMT 2000 evaluation, modified by spatial component. Scatterer positions follow from single-scattering assumption

The double-directional concept

Figure 2 is a schematic of the double-directional channel concept. Here, we distinguish between a radio channel (no directionality) and a double-directional propagation channel, which excludes the antennas. In between lies the (single-)directional channel incorporating one antenna array, as it has been known for some time. The notation of the double directional channel representation, and how it is different from simpler ones, will now be explained.

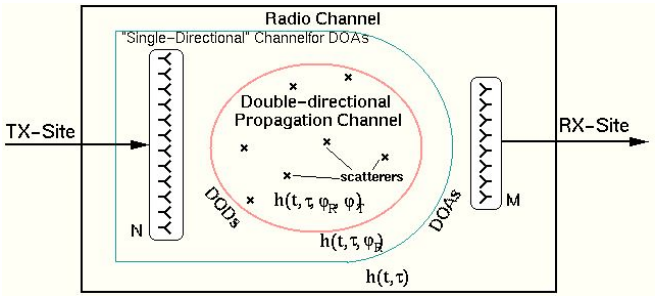

Figure 2: Double-directional channel definitions

A radio channel is usually described by complex impulse responses (CIRs) as a function of the signal delay τ. The non-directional CIR $h(\tau)$ is the angle integrated directional CIR $h(\tau, \phi_R)$

$$h(\tau) = \int_{-\pi}^{\pi} h(\tau, \varphi_R) g_R(\varphi_R) d\varphi_R \qquad (1)$$

which in turn is the angle integrated double-directional channel impulse response CIR $h(\tau, \phi_R, \phi_T)$,

$$h(\tau, \varphi_R) = \int_{-\pi}^{\pi} h(\tau, \varphi_R, \varphi_T) g_T(\varphi_T) d\varphi_T \; . \qquad (2)$$

The RX antenna system collects components from all directions, weighting them with the complex antenna pattern $g_R(\phi_R)$, and thus integrates over the respective angular domain. The TX antenna system distributes the signal-energy into the desired DODs. Valid DODs are selected from all possible directions offered by the double-directional channel for the specific propagation situation.

The double-directional channel makes visible all resolvable propagation paths between the transmitter and the receiver sites. Each path is parameterised by its excess delay τ, weighted with the proper complex amplitude $H_i e^{j\phi_i}$, and each DOD is connected to the corresponding DOA,

$$h(\tau,\varphi_R,\varphi_T)=\sum_{i=1}^{L} H_i e^{j\phi_i}\delta(\tau-\tau_i)\delta(\varphi_R-\varphi_{R,i})\delta(\varphi_T-\varphi_{T,i}). \quad (3)$$

Measurement set-up

The measurement set-up comprised a channel sounder and two antenna arrays at the RX and TX site (Figure 3). We used a RUSK ATM channel sounder manufactured by MEDAV in Germany [8]: It features 120 MHz instantaneous bandwidth and was operated at either 2 GHz or 5.2 GHz. The receive antenna array was a uniform linear array (ULA) with M_R= 8 elements half-wavelength spaced. Except for two extra, outermost elements, which served as dummies, each element was consecutively multiplexed to the single receiver train. At the transmitter side, a virtual cross-array with an omnidirectional monopole antenna excited the static channels (or a circular array on the fast-moving TX). The sounder controlled the position of the vertically polarized monopole with X-Y-stepping motors via a serial RS232 interface. Receive multiplexing avoids the cumbersome and difficult calibration of multi-channel sounders and took only milliseconds. The choice of antennas is not straight-forward. While the virtual array at one end eliminates the necessity of antenna array calibration (no mutual-coupling matrix is needed!), and facilitates arbitrary array configuration, the slow mechanical TX multiplexing requires the channel not to change noticeably during the whole measurement period. Therefore, we limited the number of positions on the cross array to M_T= 2x8=16 or used M_T= 8 linearly aligned positions. If operated, the cross array does away with forward-backward ambiguity. The monopole offers an unobstructed omnidirectional field of view for DODs, as would an ordinary MS antenna. The 2D extension of the TX array allows data extraction both in azimuth and elevation. The ULA at the receiver did limit the field of view for DOAs to some 120°, but this is not so restrictive as operative base stations (BSs) are sectorized anyway.

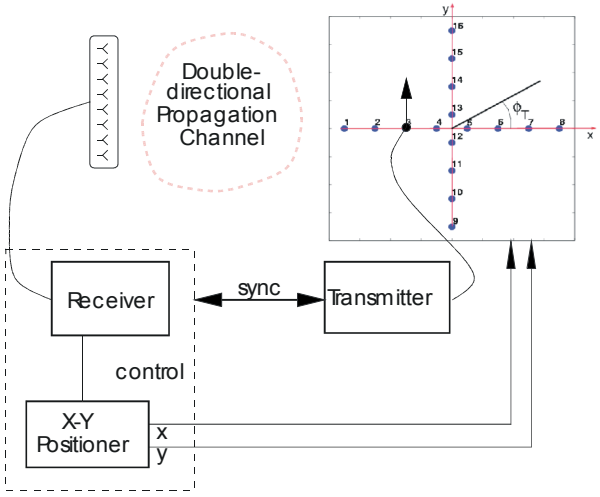

Figure 3: Measurement set-up

Estimation of DOAs and DODs

The raw data consist of $M_t \times M_f \times M_T \times M_R$ cross-multiplexed impulse responses. M_t is the number of snapshots, M_f the number of frequency samples across the 120 MHz bandwidth to obtain the averaged impulse response (see Fig. 10). These data were post-processed in several ways: by parametric estimation with Unitary ESPRIT [9] or by the conditional maximum-likelihood method (see subsection on high-speed mobiles). Unitary ESPRIT has proven its suitability for high-resolution DOA studies at the mobile station [10], [11] and at the base station [12, 13]. ESPRIT is based on a singular-value decomposition of the data matrix to arrive at its principal components that reveal the underlying signal space. It is a true superresolution algorithm, so the *number of antenna elements does not limit the angular resolution per se*. But the *number of antenna elements does limit the number of resolvable multipath components*. When the numbers M_T or M_R are small, as in our case, estimation robustness might suffer. Wideband processing compensates this shortcoming. Noise is suppressed inherently by choosing a model order less than the amount of samples.

Model order

Correct choice of the model order is crucial for the proper functioning of superresolution estimation by a subspace-based method such as ESPRIT [14] if the model order is not identified jointly within the parametric method [15]. If all incoming signals are uncorrelated, then their number is equal to the correct model order. If some signals are fully correlated, i.e. the associated wavefronts are fully coherent, then the signal space degenerates. A popular work-around is spatial smoothing [16]. Based on uncorrelated signals, we investigated several approaches for model order selection [17, 18, 19]. Most approaches return the model order correctly, provided the SNR is larger than 0 dB.

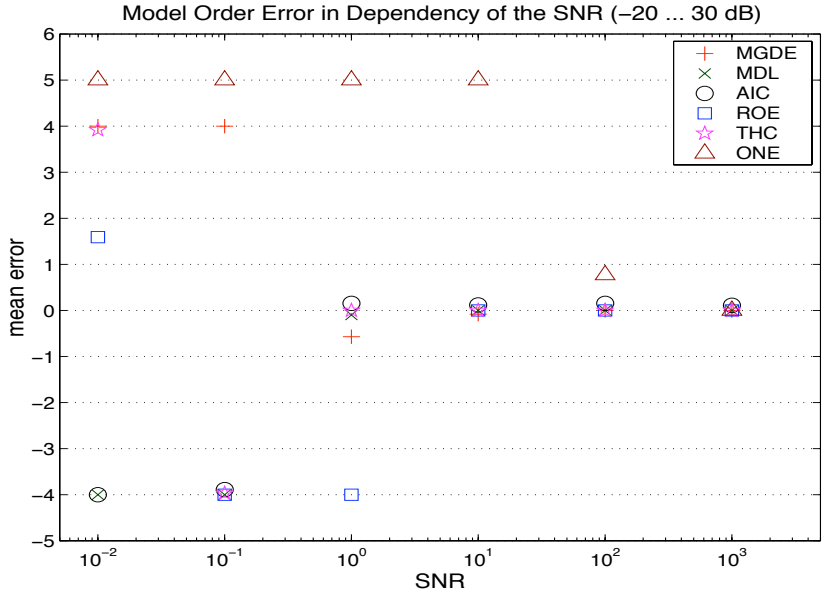

Figure 4: Model order error versus SNR (simulation: M=10 antennas, L=5 incoming signals)

Actually, the channel sounder measures, instead of impulse responses, transfer functions with typically up to 256 frequency samples for wideband characterisation. When we measure static scenarios we expect all parameters to be constant with time. For each propagation situation, we checked this and discarded measurements with Dopler frequencies other than zero. By taking M_f=192 samples of the complex transfer function, for each of the M_T antenna

positions times M_R RX antenna elements, we obtained a data set large enough to yield reliable estimates by virtue of spatial smoothing.

For the actual DOD and DOA extraction from the direct-data matrix, we devised two methods. The first one [20], [21] applies 1D Unitary ESPRIT sequentially in nested loops.

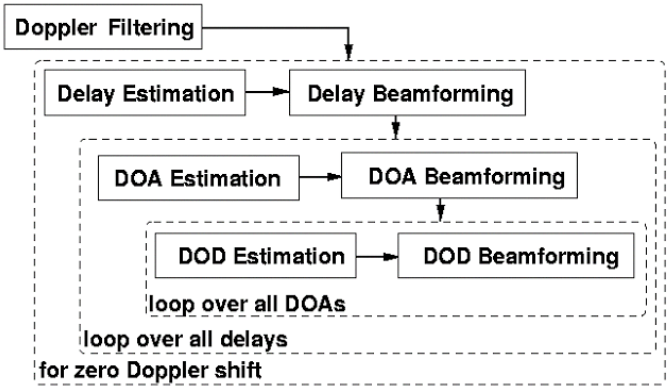

Figure 5:. Serial delay, DOA, and DOD estimation

After Doppler filtering to eliminate the possible influence of moving scatterers, propagation delay is estimated first. Delays are estimated by Unitary ESPRIT directly from the measured transfer function, as opposed to the impulse response that is obtained via windowing and Fourier transform. The associated MPC weights at each delay were obtained by beamforming with the pseudo-inverse $\mathbf{A}_\tau^+$ of the delay steering matrix,

$$\vec{h}_\tau = \mathbf{A}_\tau^+ \cdot \vec{T}_f \,, \tag{4}$$

where $\vec{h}_\tau$ is the impulse response and $\vec{T}_f$ is a vector containing the regularly spaced frequency samples. Then, DOA estimation is done; then similar beamforming to get the complex amplitudes of the waves; then DOD estimation and beamforming again. Correct pairing of parameters from concomitantly processed dimensions is established via these beamforming steps.

The second, more elegant method, exploits the shift-invariance, being the key to ESPRIT, in parallel over the different spatial and other domains (Fig. 5) [22]. By this procedure, the DOAs and DODs are automatically paired.

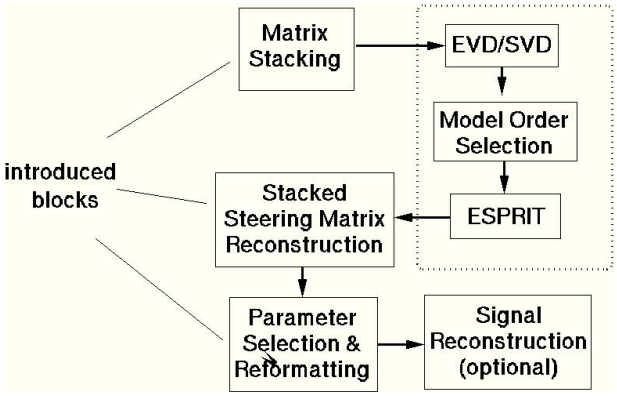

Figure 6: Joint delay, DOA, and DOD estimation

The multidimensional data matrix, properly stacked, can be fed into ESPRIT just like the one-dimensional data of usual measurements. Instead of the phase factors containing the

desired multipath parameters, we now use an intermediate eigenvector matrix to reconstruct a stacked steering matrix. Thereby, automatically combined parameters for all measured dimensions are obtained. The model order, in other approaches difficult to match over different dimensions, is also obtained in common for all dimensions.

Multipath component separation

The reasons that the mobile radio channel is dispersive in the delay, Doppler and angular domains, the latter corresponding to spatial selectivity, are different path-lengths between RX and TX sites, and position of scatterers/reflectors and their motion, respectively. So, all reasons for channel dispersion lie in the geometry of the wave propagation process, taking place via propagation paths. Evidently, *path* dispersion is generic for all kinds of dispersion. Following the *double-directional* channel concept, both the angles of arrival at the RX and of departure at the TX can be taken to separate individual multipath components. In this way, we are not limited to the assumption of single bounce by just one scatterer any more. Recently we have introduced two measures how to characterize the separability of multipath components, the MCD and the MCS [23].

If we consider only the spread between any two individual multipath components in the angular domains (DOA and DOD), then multipath component distance is

$$MCD = \sqrt{\Delta x_R^2 + \Delta x_T^2} \ . \tag{5}$$

The coordinates in this parameter space are the normalized Euclidian distance between two points on a unit circle characterizing either the DODs ($\rightarrow \Delta x_T$) or the DOAs ($\rightarrow \Delta x_R$). The normalization is such that the maximum of either coordinate is unity and its minimum is zero (Fig. 7).

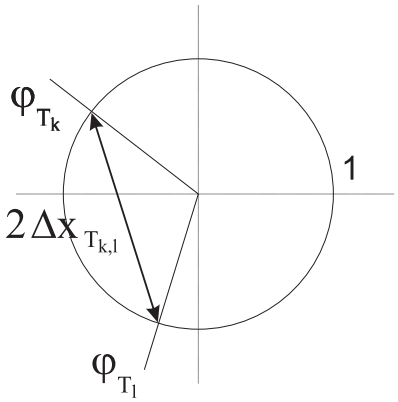

Figure 7: Definition of normalized angular separation

A global measure for a specific environment under investigation is the *multipath component separation* (MCS), being the power-weighted mean of all individual MCDs,

$$MCS = \sqrt{\sum_k^N \sum_l^N MCD_{k,l}^2 P_{k,l} \Big/ \sum_k^N \sum_{l \neq k}^N P_{k,l}} \ . \tag{6}$$

The cross-power $P_{k,l} = \sqrt{P_k P_l}$ of paths k,l restricts the influence of low-power paths. Note that the sum can be extended over all multipath components (MPCs) since the k-th component has no contribution ($MCD_{k,k}$ =0). The higher the power of the paths to be separated the larger the MCS.

Figure 8 shows the ccdf of the MCD for a sample scenario with just two paths: at Position B there is large MCD and at Position A there is low MCD. The two-dimensional MCD we defined before is the squared sum of these, MCD_A and MCD_B.

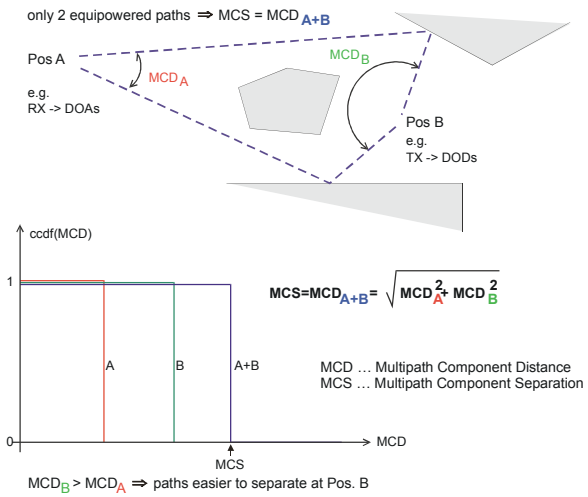

Figure 8: Simplified sample scenario with two equipowered paths to demonstrate multipath component distance and separation

The features of the MCS are i) it is system-independent and as such appropriate to characterize different environments for a variety of candidate systems; ii) it can be extended to account for several dimensions. First, the elevation would be interesting in a scenario in which the MPCs arrive from angles with elevation other than zero ([11]). Further extensions include separation of MPCs in delay [23], or, in a highly dynamic scenario, the Doppler shift as further coordinates in the parameter space of MCD; iii) it combines the spreading in all considered physical dimensions into one single figure-of-merit.

The MCS tells us whether there are many dominant multipath components available at either end of the link that are useful to look at individually. A word of caution is in place if we want to use delay and/or Doppler as a parameter to separate MPCs. As we will show in the next paragraph, delay is suitable to separate two MPCs impinging via the same DOA, but it is actually their different DODs that increase MIMO data transmission capacity [24].

An interesting use of the MCS would be answering the question whether it is more useful to opt for beamforming or diversity processing. If we have only one array at our disposal, the MCDs will have no contribution from the other (omni-directional) site. The corresponding MCS then tells where to put the array – at the location with the higher value of this MCS. In an actual deployment of a MIMO system, the (joint) multipath component separation MCS helps in estimating the performance that will be achieved. Note, that from the viewpoint of MCS, the measured positions of RX and TX antenna arrays as potential BS and UE sites are important, but not whether you place, in the measurement, TX or RX there.

Do the measurement results give information on MIMO capacity? Not directly, because our measurements yield a single realization of the stochastic channel at each site. But to make predictions about MIMO channel capacity one can proceed as outlined in [25]: To obtain different realizations of the channel one can ascribe a random phase to each multipath component. This phase is chosen independent for each multipath component, but completely correlated for all antenna elements. Repeating the procedure with different phases for the multipath components gives an ensemble of channel and capacity realizations.

Sample results

We will now show a double-directional measurement in an office environment (NLOS) in Vienna, Austria, at 2 GHz, and in an open yard (LOS) in Ilmenau, Germany, at 5.2 GHz.

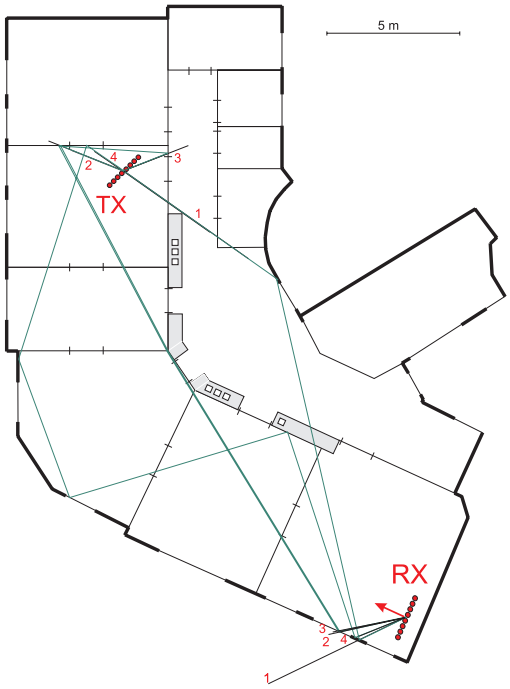

	τ [ns]	DOA [°]	DOD [°]
1st path	73,2	44	-11
2nd path	82,5	32	147
3rd path	95,4	31	-66
4th path	113,2	40	170

Figure 9: Office environment in Vienna with the four strongest propagation paths.

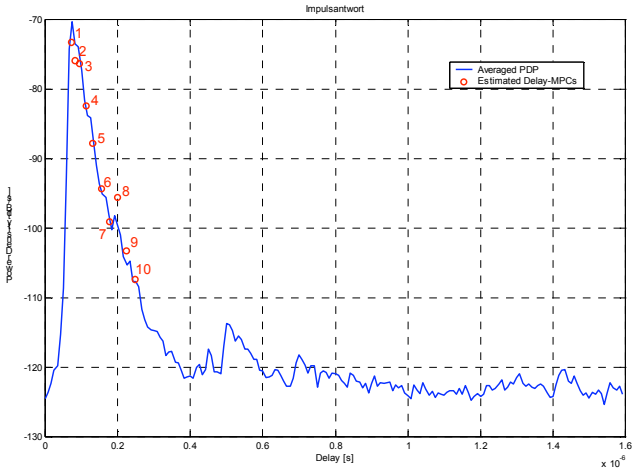

Figure 10: Averaged impulse response in office environment

The office (Figure 9) was furnished with predominantly wooden furniture. The outer walls were heavy brick, the inner walls plaster board with low attenuation. The measured and averaged impulse response is shown in Figure 10 as a continuous blue line.

The seemingly high dynamic range is a consequence of the averaging. The red circles are estimates of the incident waves (MPCs) at the receiver. Although the basic data are the same, the excellent agreement of measured and estimated MPCs is not self-evident. Coming back to Figure 9, we have included the four strongest paths and their most probable traces. There are at least two reflections/scatterings between TX and RX.

Figure 11: Open yard

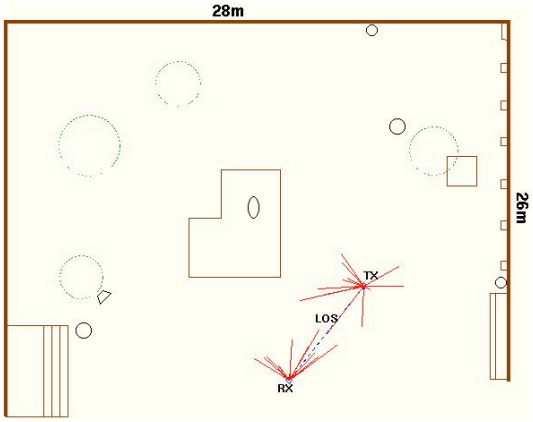

Figure 12: Top view of open yard

Figure 11 gives an impression of the open yard in Ilmenau, where the 5GHz measurements were taken. In the left-hand foreground there is the receive array, in the right-hand foreground the channel sounder. The TX antenna and the absorber to shield it from the metal structure of the x-y-table can be seen in the background. A map of this environment is shown in Figure 12, the impulse response in Figure 13.

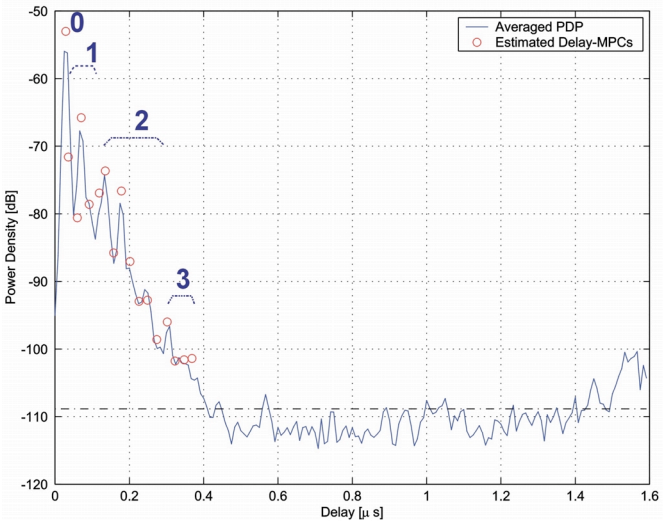

Figure 13: Averaged impulse response in open yard

The strongest path by far (the length of the DOAs and DODs in Figure 13 are scaled in dB), is the LOS line-of-sight path, as could be expected. Interestingly, there are many other paths, probably a consequence of the many scatterers and trees around, but we could not trace them unambiguously. Still, in Figure 13 they come out clearly and distinctly.

Measurements for high-speed mobiles

So far, all the channels that we have described were stationary. In fact, this was a consequence of our using a virtual linear or planar array at one end of the radio link. To demonstrate that stationarity is not an inherent limitation of the double-directional measurement approach, we performed a trial that focused on the time-variance introduced by a mobile station moving at high speed. In this trial, the double-directional channel parameters

for the arrival- and departure angles were estimated using, at the TX, a 15-element uniform circular array of monopoles mounted on a ground plane (Fig. 14) on top of a car driving at 160 km/h ("UCA-15", spacing 0.43 wavelength).

Fig. 14: Circular antenna array for high-speed measurements

The RX used the uniform linear array of 8 patch elements already mentioned ("ULA-8", spacing 0.5 wavelength), and was at a fixed position. The individual channel transfer functions between all 15x8 pairs of transmitting and receiving antenna elements are measured in a total bandwidth of 120 MHz.

The DOAs and DODs are estimated by a Conditional Maximum-Likelihood Estimator (CMLE). This choice of algorithm is motivated by the effective "spiral" geometry of the moving uniform circular array. The circular array moves during the time-multiplexed measurements of the individual transfer functions associated with pairs of transmit and receive elements. The effective array geometry is deformed from the ideal circle to a spiral. Numerically efficient estimators (e.g. ESPRIT, Root-MUSIC) based on algebraic methods are not known to the authors for this type of geometry. Algorithms which can cope with arbitrary element positions rely on search techniques. The CMLE is one of the simplest to implement and has considerably lower numerical complexity than the Maximum-Likelihood Estimator (MLE) for several wavefronts carrying stochastic signals. For further details, we refer to [26].

Let $\boldsymbol{H}_k$ be the observed channel transfer matrices for several snapshots $k = 1,\ldots, K$ at a selected delay-bin τ. Further, the two transmitter- and receiver-side covariance matrices are estimated via the usual sample-averages

$$\hat{\mathbf{C}}_R = \frac{1}{K}\sum_{k=1}^{K} \mathbf{H}_k \mathbf{H}_k^H, \;\; \hat{\mathbf{C}}_T = \frac{1}{K}\sum_{k=1}^{K} \mathbf{H}_k^H \mathbf{H}_k^*. \tag{7}$$

Let $\boldsymbol{d}_T(\phi_T)$ and $\boldsymbol{d}_R(\phi_R)$ denote the steering vectors of the transmitter- and receiver-side, respectively, where ϕ_T is the DOD and ϕ_R is the DOA. These steering vectors span the signal spaces on both sides of the multiple-input, multiple-out mobile radio channel. Let the projection matrices of the associated signal spaces be denoted by $\boldsymbol{P}_T(\boldsymbol{\theta}_T)$ and $\boldsymbol{P}_R(\boldsymbol{\theta}_R)$. Here, we have defined the DOD parameter vector $\boldsymbol{\theta}_T$ of dimension S which contains the S distinct DODs, and analogously for the DOAs in $\boldsymbol{\theta}_R$.

Finally, the conditional log-likelihood function for the DODs can be formulated as

$$L_T(\theta_T) = -\log\mathrm{tr}[\mathbf{P}_T(\theta_T)^{\perp}\hat{\mathbf{C}}_T], \tag{8}$$

where $(.)^{\perp}$ denotes the orthogonal complement, i.e.

$$\boldsymbol{P}_T(\boldsymbol{\theta}_T)^{\perp} = \boldsymbol{I} - \boldsymbol{P}_T(\boldsymbol{\theta}_T). \tag{9}$$

The conditional log-likelihood function $L_R(\boldsymbol{\theta}_R)$ for the DOAs in $\boldsymbol{\theta}_R$ takes the same form with all subscripts "T" replaced by "R". The goal functions $L_R(\boldsymbol{\theta}_R)$ and $L_T(\boldsymbol{\theta}_T)$ can be maximized in an iterative way [27]: This is explained in the following for the DOD only. In a first step, we assume that only one path is present: $\dim(\boldsymbol{\theta}_T^{(1)})=1$. We do a global grid search over all ϕ_T. Having found the maximizer $\phi_T^{(1)}$ of $L_T(\boldsymbol{\theta}_T)$, we set $\boldsymbol{\theta}_T^{(1)} = (\phi_T^{(1)})$. We proceed by null-projection the associated signal estimate,

$$\widetilde{\boldsymbol{C}}_T = \boldsymbol{P}_T(\boldsymbol{\theta}_T)^{\perp} \hat{\boldsymbol{C}}_T \boldsymbol{P}_T(\boldsymbol{\theta}_T)^{\perp}. \tag{10}$$

Next, we assume that exactly two paths are present, $\dim(\boldsymbol{\theta}_T^{(2)})=2$, and a global grid search over all DODs $\phi_T^{(2)}$ is carried out with fixed $\boldsymbol{\theta}_T^{(1)}$. Having obtained two DOD estimates for these two paths by independent global search runs, we need to refine these by a subsequent *joint* optimization. Here, it suffices to use a few steps of a local optimization procedure. For the purposes of this paper, we used the BFGS-algorithm which is named after Broyden, Fletcher, Goldfarb, and Shanno.

Estimation results from the CMLE are shown in Figure 15.

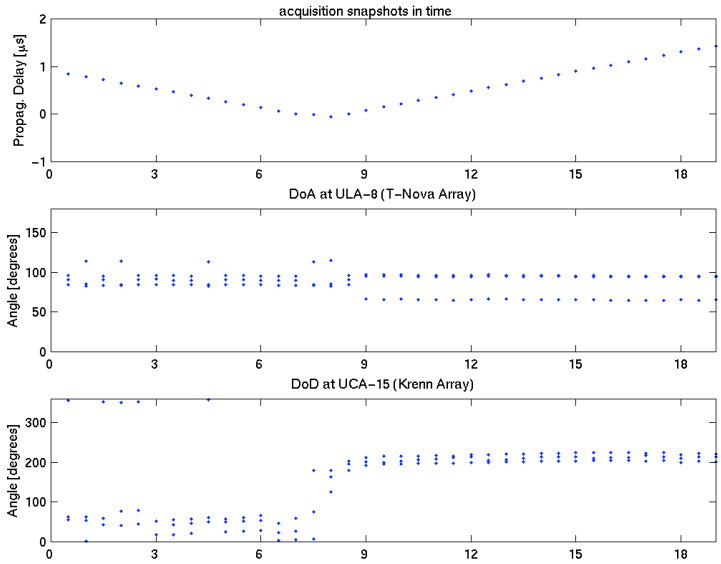

Fig. 15: Delay, DOA, and DOD of the identified paths over time in seconds

At the top of Figure 15, the estimated path delays between transmitting car and receiving array are shown over time. In the middle, the DOA estimates at the linear array are shown over time as the car moves at approximately 160 km/h past the receiving array. Several arrivals can be identified. At the bottom, the estimates for DoD at the circular array are shown: a clear trajectory of the DoDs is visible.

Discussion

It has become customary to establish MIMO capacity by eigenvalue decomposition of the channel matrix [28]. For analysis, this method gives a good impression about the achievable ergodic capacity. However, the number and the arrangement of the TX and RX antennas

enter critically in the analysis. Extrapolation to other antenna systems is not straight-forward, because the antennas are an integral part of the MIMO system under scrutiny. In our double-directional approach, the antennas are not part of the propagation channel, so the result is independent of the number, arrangement, etc of the antennas used. So, for synthesis, and for roll-out of a MIMO system or a smart antenna use double-directional measurements instead. Then you have the most detailed information at hand about the environment where you want to deploy the system. Such initial double-directional (DD) measurements will also aid in assessing where to place exactly a smart antenna for optimum benefit. MIMO systems can enhance transmission capacity, but they also can provide diversity of high order [29]. A DD measurement will tell you whether to expect either or both: when the MCS is large, beamforming, e.g., can be used to boost capacity, when the MCS is small, you might benefit mostly from diversity.

We envisage a site-specific deployment of smart antennas and MIMO systems. Smart antennas are employed, among other reasons, for their capability to reduce interference. As the directions of departure are more or less discrete, our approach opens an interesting new possibility to improve system performance. Send only in the DODs that lead to valid DOAs! Otherwise your costly power will not reach the receiver anyway and you will waste it. Furthermore, if you design your radio links such that power is not spilled in any arbitrary direction where it will contribute to interference power, system SINR will be improved. This relieves the burden upon the receivers to suppress interference.

To install a MIMO system, you will have antenna arrays available at both link ends anyway. We envisage an initial test measurement of the kind described in this paper, to obtain the main propagation directions. Once you have those determined, then shaping your beam pattern accordingly is a task well known to antenna engineers. In his doctoral dissertation [30], Jochen Hammerschmidt has recently taken up this issue again and shown, how easily, albeit effectively, multiple beams can be formed by a few antenna elements via grating lobes utilized in smart antenna designs.

Acknowledgements

We gratefully acknowledge the provision of the eight-element linear patch array by Ingo Gaspard of T-Nova, Darmstadt, Germany. We would like to thank Arpad Scholtz and Hermann Anegg for their support in antenna design and measurements. The authors would like to thank Manfred Lenger for his ideas on high speed measurements. The measurements and analysis for high-speed mobiles were supported by the Wiener Wirtschaftsförderungs-fonds and Siemens PSE PRO RCD through the ftw. project C2 “smart antennas” which was carried out by INTHF, ftw., Austrian Research Centers Seibersdorf, and Siemens PSE PRO RCD. We are grateful to Prof. Reiner Thomä and his group (Dirk Hampicke, Gerd Sommerkorn, Axel Schneider, Andreas Richter, Uwe Trautwein) at TU-Ilmenau for enabling the first measurement campaign and for their help throughout the measurements. We thank our colleagues Martin Toeltsch, Hüseyin Özcelik, and Plamen Dintchev for the evaluation of data and preparation of figures. Finally, we are grateful to Ralf Müller, ftw., who pointed out that scatterer separation in time-delay cannot be exploited for enhancing MIMO capacity.

References

[1] P. Pajusco, Experimental Characterization of DOA at the Base Station in Rural and Urban Area, Proceedings of the IEEE Vehicular Techn. Conf. 1998 (VTC'98), pp. 993-997, 1998.

[2] H. Bölcskei, D. Gesbert, and A. Paulraj, On the capacity of OFDM-based Spatial Multiplexing Systems, IEEE Trans. Comm., in press

[3] J. Bach Andersen, Constraints and Possibilities of Adaptive Antennas for Wireless Broadband, Proc. 11th Int. Conf. Antennas and Propagation, 17-20 April,2001, Manchester, UK, IEE Publication No. 480, pp 220 – 225

[4] P.A. Bello, Characterization of Randomly Time-variant Linear Channels, *IEEE Trans. on Communication Systems*, vol. CS-11, pp. 360-393, 1963.

[5] M. Steinbauer, "The Directional and Double-directional Radio Propagation Channel', PhD Thesis, October 2001, TU-Wien

[6] R. Kattenbach, Charakterisierung zeitvarianter Indoor-Funkkanäle anhand ihrer System- und Korrelationsfunktionen, PhD Thesis, Universität-Gesamthochschule Kassel, 1997, Shaker Verlag, ISBN 3-8265-2872-7.

[7] ITU-Recommendation, Guidelines for Evaluation of Radio Transmission Technologies for IMT-2000, Rec. ITU-R M.1225, 1998.

[8] R. Thomä, D. Hampicke, A. Richter, G. Sommerkorn, A. Schneider, U. Trautwein and W. Wirnitzer, "Identification of Time-Variant Directional Mobile Radio Channels", IEEE Trans. on Instrumentation and Measurement, **49**(2):357-364, April 2000.

[9] M.Haardt and J.A.Nossek, "Unitary ESPRIT: How to obtain increased estimation accuracy with a reduced computational burden", *IEEE Transactions on Signal Processing*, **43**(5):1232-1242, May 1995

[10] J. Fuhl, J.P. Rossi and E. Bonek, "High-resolution 3-D Direction-of-Arrival Determination for Urban Mobile Radio", *IEEE Transactions on Antennas and Propagation*, **45**(4):672-682, April 1997

[11] A. Kuchar, J.-P. Rossi and E. Bonek, Directional Macro-Cell Channel Characterization from Urban Measurements, IEEE Trans. on Antennas and Propagation, vol. AP-48, no. 2, pp. 137-146, Feb 2000.

[12] U. Martin, A Directional Radio Channel Model for Densely Built-Up Urban Areas, Proceedings of the 3rd European Personal Mobile Communications Conference (EPMCC'97), pp 237ff, 1997, (also in IEE Proc. of Radar, Sonar and Navigation, Special Issue on antenna Array Processing Techniques)

[13] J. Laurila et al., "Wideband 3-D characterization of Mobile Radio Channels in Urban Environment", IEEE Trans. Antennas & Propagation, in press

[14] R. Roy, T. Kailath, ESPRIT – Estimation of Signal Parameters via Rotational Invariance Techniques, IEEE Trans. on Acoustics, Speech, and Signal Processing, vol. ASSP-37, pp. 984-995, July 1989.

[15] C.F. Mecklenbräuker, P. Gerstoft, J.F. Böhme, P.-J. Chung: "Hypothesis testing for geo-acoustic environmental models using likelihood ratio", J. Acoust. Soc. Am., **105**(3):1738-1748, March 1998.

[16] T.J. Shan, M. Wax and T. Kailath, On Spatial Smoothing for Direction-of-Arrival Estimation of Coherent Signals, *IEEE Trans. On Acoustics*, *Speech and Signal Processing*, vol. ASSP-33, pp. 806-811, 1985.

[17] H.Wu, J. Yang, F. Chen, "Source number estimators using transformed Gerschgorin Radii", *IEEE Transactions on Signal Processing*, **43**(6):1325-1333, June 1995

[18] J. Fuhl, "Smart Antennas for 2nd and 3rd Generation Mobile Communications Systems", Doctoral Dissertation, Technische Universität Wien, July 1997.

[19] M. Wax and T. Kailath, "Detection of signals by information theoretic criteria", *IEEE Transactions on Acoustic, Speech, and Signal Processing*, **33**(2):387-392, April 1985.

[20] M. Steinbauer, D. Hampicke, G. Sommerkorn, A. Schneider, A. F. Molisch, R. Thomä and Ernst Bonek, Array Measurement of the Double-directional Mobile Radio Channel, Proc. of IEEE Vehicular Technology Conf. 2000 (VTC'2000) – Spring, Tokyo, May 2000.

[21] M. Steinbauer, A.F. Molisch, E. Bonek, The Double-directional Radio Propagation Channel, IEEE Antennas and Propagation Magazine, August 2001.

[22] Patent applied for

[23] E. Bonek et al., Double-directional Radio Channel Measurements – What We Can Derive from Them, Proc. Int. Symposium on Signals, Systems, and Electronics (ISSSE 01), Tokyo, Japan , July 24-27, 2001.

[24] Müller, private communication.

[25] A.F. Molisch, M. Steinbauer, M.Toeltsch, E.Bonek, and R.Thomä, Capacity of MIMO Systems Based on Measured Wireless Channels, IEEE Journal on Selected Areas in Communications (JSAC), accepted for publication, 2001.
[26] J. F. Böhme, Array processing in S. Haykin (Ed.), Advances in Spectrum Analysis and Array Processing, Vol. I, Prentice–Hall, Englewood Cliffs, NJ. pp.1-63, 1991.
[27] R.H. Shumway, Replicated Time-Series Regression: An Approach to Signal Estimation and Detection, in D. Brillinger and P. Krishnaiah (Eds.), "Handbook of Statistics", Vol. 3, Elsevier Science Publishers B.V., pp. 383–408, 1983.
[28] A.G. Burr, Capacity of Multi-element Transmit/receive Antenna (MIMO) Wireless Communication Systems, Technical Report C0, Forschungszentrum Telekommunikation Wien (ftw.), 1999.
[29] J. Bach Andersen, Antenna Arrays in Mobile Communications: Gain, Diversity, and Channel Capacity, *IEEE Antennas and Propagation Magazine*, vol. 42, no. 2, pp. 12-16, April 2000.
[30] J.S. Hammerschmidt, "Adaptive Space and Space-Time Signal Processing for High-Rate Mobile Data Receivers", PhD Thesis, Technische Universität München, June 2000.